IJCRT.ORG ISSN : 2320-2882

INTERNATIONAL JOURNAL OF CREATIVE RESEARCH THOUGHTS (IJCRT)

An International Open Access, Peer-reviewed, Refereed Journal

Design and Development of Magneto Rheological Fluid Base Damper

Mr. Rahul Bhatu Vendait [#1], Prof. R R Kulkarni [*2], Prof. B B Kedar[*3]

[#1] *PG Student, Department of Mechanical Engineering, Siddhant COE, Sudumbre, SPPU, Pune, India.*

[*2,3] *Assistant Professor, Department of Mechanical Engineering, Siddhant COE, Sudumbre, SPPU, Pune, India.*

Abstract

Over the past three decades, a great deal of interest has been generated regarding the use of structural protective systems to mitigate the effects of dynamic environmental hazards, such as vibration, on mechanical engineering structures and automobile sectors for human comfort, earthquakes and strong wind, on civil engineering structures. These systems usually employ supplemental damping devices to increase the energy dissipation capability of the protected structure. One of the most promising new devices proposed for structural protection is magneto rheological (MR) fluid dampers. MR fluids possess rheological properties, which can be changed in a controlled way. These rheological changes are reversible and dependent on the strength of an excitation magnetic field. MR fluids have potentially beneficial applications when placed in various applied loading (shear, valve and squeeze) modes. Magneto rheological dampers, or as they are more commonly called, MR dampers, are being developed for a wide variety of applications where controllable damping is desired. MR fluid dampers have the capability of changing their effective damping force depending on the current input to the damper. These applications include dampers for automobiles, heavy trucks, prosthetic limbs, gun recoil systems, bicycles, and possibly others related to mechanical discipline like brake, clutch etc. Magneto rheological (MR) fluid dampers having very good mechanical simplicity, high dynamic range, low power requirements, large force capacity, and robust ness, this class of devices has been shown to mesh well with application demands and constraints to offer an attractive means of protecting infrastructure systems. This work issues the design and analysis of the linear magneto rheological damper. Basic information concerning the characteristics of the typical magneto rheological fluid and the damper incorporating it, were presented with the detail description of the applied fluid developed in our premises. With reference to the computations, the prototype damper was designed, manufactured and tested under different operating conditions. Performed calculations were verified with the experimental results and their accuracy was evaluated. The conclusions and observations from the research were compiled in the summary.

Keywords: Vibration, magneto rheological fluid dampers, loading modes, Automobile.

I. INTRODUCTION

People are most sensitive for vertical vibrations between 5 & 16 Hz & to the lateral vibration between about 1 & 2 Hz. Women are more sensitive than men to vertical vibration above about 10 Hz. Most responses of seated subjects implicated the lower abdomen at 2 Hz moving up to body at 4 & 8 Hz, with most responses implicating head at 16 Hz. At 32 Hz the responses are divided between the head & lower abdomen [2]. It is seen that often trade-offs influence the design process of any item. The design process of automotive suspension system is also not the exception from this. The general trade-off between ride comfort and vehicle stability is the motive for advancements in design of automotive suspension systems. Measurement of ride comfort is subjective but it can be quantified by the amount of energy transmitted through the suspension into the passenger compartment (sprung mass). Ride quality is derived closely with respect to the acceleration of the sprung mass [2]. Passengers feel few road disturbances in a Cadillac vehicle and this is a good example of this kind. Opposite to this, passengers feel many of the road disturbances transmitted by a Corvette's suspension which has higher vehicle stability. Vehicle stability is also known as road holding ability. Compared to a Cadillac, a Corvette is a much more manoeuvrable vehicle and holds the way appreciably better. In an ideal world, a vehicle suspension would react just as to aggressive driving as it does to highway cruising. The objective of this discussion is to emphasis the approach towards this ideal concept. Spring and damper are two critical components for a specific suspension vehicle. Weight of the vehicle is an exclusive important selection criterion for spring whereas suspension's placement on the compromise curve is mainly determined by damper. Damper selection is mainly governed by type of vehicle keeping the performance of vehicle at its optimum level. Theoretically, passengers should not be affected by low-frequency road disturbances when dampers are used. At the same time, dampers must absorb high-frequency road disturbances. When high damping effect is achieved, ideally passengers do not have any effect of low-frequency road disturbances. However, this situation leads to absorb high- frequency at very poor rate. If damping effect is made low, this situation leads to absorb high-frequency at very good rate but this is achieved at the cost of low-frequency isolation. In the field of automotive suspensions, many innovative and improved concepts are emerged due to requirement to reduce the effect of this trade-off.

Following types of suspensions are reviewed here :(i) Passive (ii) Fully active (iii) Semi-active

The conventional passive suspension system consists spring and damper. Spring is used to store the energy in suspension and at the same time, damper is used to dissipate the energy. Both components are finalised at design stage only. Due to this, this type of suspension is paralysed and known as classic suspension compromise. Interchanging force actuator with damper, suspension is converted into fully active suspension. However, looking to the constraints like difficulty in operation and higher power utilisation, fully active suspensions are not yet coming in regular use. The basic concept for fully active suspension is to apply the force either in the form of jounce or in the form of rebound to suspension using force actuator. Such force is dynamically monitored and controlled by the control system integrated in the suspension itself. Various control systems will be narrated later in this thesis. Semi-active suspension is last (third) type of suspension and same is discussed further. In this type, passive damper is interchanged with a semi-active damper which is having the potential to change the damping characteristics. This type of damper has also the ability to offer wider band of damping using mechanically controlled orifices or by monitoring and controlling fluid viscosity. It should be noted that damping value is changed in accordance with control algorithm used. An exhaustive literature review is carried out to understand the present practices and theories in damper design. It will also help to obtain a better understanding of how individual internal components and internal flows had been designed and modelled in the past.

Problem Definition:

- To understand basics of the force- displacement, force-velocity and force-time behavior of a new magneto-rheological (MR) fluid damper.
- To develop a theoretical study to predict behavior of new MRF dampers; and
- To conduct a comprehensive experimental study on the proposed MRF damper to validate all theoretical results.

This study aims design, fabrication and characterization of an MRF damper with design and fabrication of test rig for characterization of developed damper.

Objectives of the work:

The primary objectives of this research are:

1) To develop the MR fluid for application of damper
2) To conceptually design an MR damper
3) To develop the prototype of the MR damper
4) To evaluate the performance of the MR damper experimentally.

Scope of work:

1) Understand basic theory of vibration
2) Understand MR fluid basics, behavior, production and applications in various fields as a smart fluid
3) Understand various designs which are commonly used for MR dampers.
4) Develop design alternatives from existing MR damper designs.
5) Design of the prototype damper
6) Prototype fabrication of improved design MR damper
7) Design and fabrication of test rig for testing damper
8) Testing of the newly developed damper for optimization
9) Comparison of MR damper with conventional damper

Data analysis is carried out with the help of statistical software like Design Expert, ANOVA and EXECL (MS OFFICE) with C programming whenever needed.

II. LITERATURE REVIEW

An exhaustive literature review is carried out to understand the theories and present practices in magneto rheological (MR) fluid and damper design. It will help to obtain a better understanding how MR fluid behaves under different mode of applications. It will also help to obtain a better understanding how the individual internal components and internal flows in damper had been designed and modelled in the past. This section presents background information on MR fluid and damper technology. The information here is a summary of important information found in a comprehensive literature review. Journal articles, thesis and books were searched for topics relating to controllable fluids like MR fluid, Magnetisable Particles, Carrier Fluid and additives, Magnetic properties of MR fluids, off state viscosity, Basics of Rheological Properties yield stress, B-H Relationship, Durability and In-Use-Thickening shock absorbers, dampers, active damper, magneto rheological dampers and its properties with rheological aspects like Off and On State Rheology, Operating Modes of MR-Fluids, vole mode, direct shear mode, squeeze and pinch mode, Volume Fraction and Particle Size Factors, MR damper models, Probability models and stochastic models. Application of MR fluids in dampers and shock absorber, breaks and clutches were discussed. Each result of this search was examined for relevance to the subject.

III. DESIGN AND MANUFACTURING

Quasi-Static Modeling For MR Dampers

This chapter presents two quasi-static models namely axisymmetric & parallel-plate model, based on the NavierStokes equation are established for MR damper behavior. The Herschel-Bulkley visco-plasticity model is used to define the MR fluid field-dependent features and shear thinning/thickening effects. Simple equations created on these damper models are given which can be used in the initial design phase. Effects of geometry on Controllable force, dynamic range and MR damper performance are also discussed.

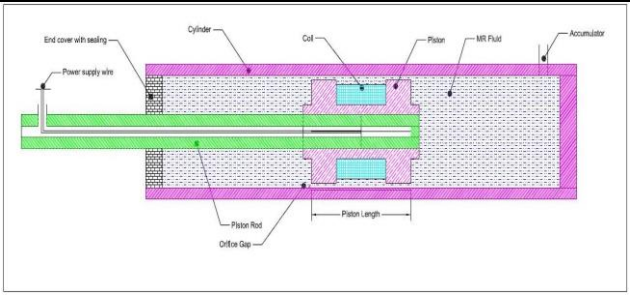

Figure 1:Schematic of small scale MR fluid damper

Following assumptions are made for quasi-static analysis of MR fluid dampers:

1) MR fluid flow is fully developed
2) MR dampers move at a constant velocity; and
3) The Herschel-Bulkley visco-plasticity model is applied to describe MR fluid field-dependent characteristics and shear thinning/thickening properties.

To interpretation for the fluid shear thinning or thickening influence, the Herschel-Bulkley visco-plasticity model is employed. In area I, the shear strain rate $\gamma^{\cdot} = dux/dr \geq 0$.

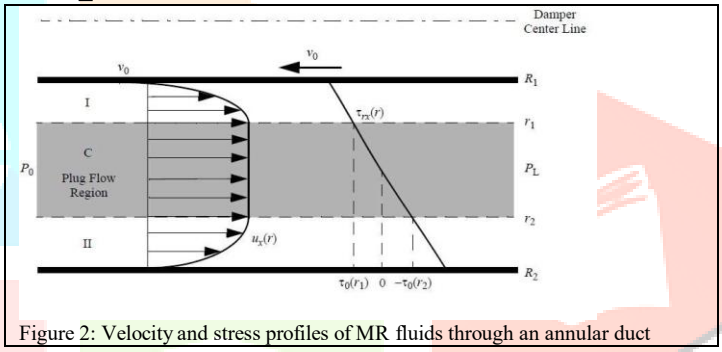

Figure 2: Velocity and stress profiles of MR fluids through an annular duct

Further the Herschel-Bulkley model is reduce to the Bingham visco-plasticity model while the fluid parameter m = 1.

MR Damper Design and Fabrication

The MR fluid has been prepared using mechanical stirrer. The electronic weighing machine is used to measure the amount of additives required in the composition. Initially the mixture of carrier fluid and additive is prepared and stirred for 4 hrs. The amount of carbonyl iron particles as mentioned in Table are then added into the prepared mixture and stirred for 72 hrs. The magneto rheological fluid, developed in house, is used in the prototype damper. The fluid is a suspension of a 4 to10 micron diameter sized magnetically susceptible particles mixed in Castor oil carrier fluid. According to the data available by testing this MR fluid on rheometer at this laboratory, the density of the liquid is around 3 gm/cm^3 and off state viscosity of a 3.5 Pa-s. The maximum yield stress value is 15 kPa and it is achieved with the magnetic induction of 0.7 T. As soon as exposed to a magnetic field, the rheology of the fluid reversibly and instantly alterations from a free-flowing liquid to a semi-solid state with the controlled yield strength as a consequence of the sudden change in the particles arrangement.

TABLE 1: Properties of MR fluid used for present investigation.

Property	**Value**	**Property**	**Value**
Appearance	Dark Gray Liquid	Solid particles	Iron particles having 4-10 micron size
Off State Viscosity (at 33 ^{0}C)	3.5 Ps (Pascal-second)	Maximum Yield Stress	@ 5000 N/m^2 at 0.75 T
Density	3 gm./cm^3	Response time	Some millisecond
Solid Contains by Weight	40%	Stability	Good for most impurities
Flash Point	> 140 ^{0}C	Relative permeability of MR Fluid	6 H/m
Operating Temperature	-30 to 120 ^{0}C	Saturation Magnetic	0.75 T
Carrier fluid	Castor Oil		

MR Damper Geometry Design

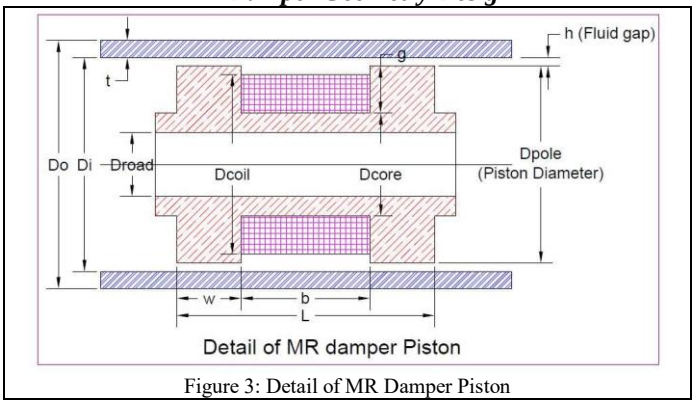

Figure 3: Detail of MR Damper Piston

The MR damper geometry design is started by assuming following parameters:

(1) MR fluid yield stress r_0, and fluid factors K and m
(2) MR damper dimension Di (i.e. Inner Diameter of Housing)
(3) Maximum permissible velocity of the MR damper

Table II: the terminology used during discussion for MR fluid base damper geometric design.

Diameter of piston	D_p	Core Depth	g
Length of Piston	L	Area of Piston Annulus	A_{pa}
Width of Piston pole	w	Area of Fluid Annulus	A_{fa}
Diameter of Road	D_r	Core Area	A_{core}
Core Diameter	D_{core}	Path Area	A_{path}
Cylinder Inside Diameter	D_i	Pole Area	A_{pole}
Core Width (Length of Coil)	b	Number of Turns of Piston Coil	N
Thickness of cylinder	T	Vacuum Permeability	μ_0
Cylinder Outside diameter	D_o	Relative permeability of Piston	μ_{rp}
Fluid gap	h	Relative permeability of Cylinder	μ_{rc}
Radius of Fluid Annulus	R_{fa}	Relative permeability of MR Fluid	μ_{MR}
Saturation Magnetic Induction for MR Fluid.	BS_{MR}	Saturation Magnetic Induction for Piston.	BS_p
Ratio of shear stress and magnetic induction	C_{cB}	Saturation Magnetic Induction for Cylinder.	BS_c

The geometry design of MR damper is to select a suitable gap dimension *h* and active pole length L such that the design requirements of "dynamic range" D and controlled force Fc, are attained. The controllable force and the dynamic range are two of the most important parameters in evaluating the overall performance of the MR damper.

The design procedure for a magnetic circuit is carried out in following step:

To find out the magnetic induction B_f in the MR fluid to make availablerequired yield stress r_0.

(1) To find out the magnetic field strength H_f in the MR fluid.
(2) The total magnetic induction flux.
(3) To find out the magnetic field intensity H_s in the steel.
(4) With the help of Kirchhoff's Law of magnetic circuit, the required number ofamp-turns (NI).

Additional things should also be keep in mind throughout the circuit design process such as nonlinear magnetic properties of piston & cylinder material and MR fluid; probable losses at boundaries & junctions; limits on voltage, current and inductance; probable inclusion of permanent magnets for reliable action and eddy currents. To finalize outstanding magnetic material and MR fluid is the main step of magnetic circuit design to the fulfilment of design intent. Better magnetic design is also carried out by magnetic structure design. The magnetic field forms a loop in the magnetic material. If the magnetic loop gets saturate anyplace, it will stop the continuous rise of the entire loop. However at the same time, the magnetic structure must confirm the execution of structure function.

The complete magnetic circuit design is carried out in following steps.

Step 1: Calculation of magnetic reluctance for damper circuit.
Step 2: To find out optimum magnetic flux for MR damper circuit (ϕ):

Step 3: To find out Optimum (Maximum) current value which can produce magnetic induction in circuit (I_{max})

TABLE III. Magneto rheological Damper Working Dimensions

Damper Parameter	Dimension (in mm)
Total length (extended)	620
Total length (compressed)	300
Maximum stroke length	320
Mid stroke length	460
Inside shock tube diameter	44.55
inner/outer eyelet diameter	24/55

Figure4: Designed and fabricated for the research experiment

Components of the Designed MR Dampers

The damper of the current experiment is represented in Figure, The damper is fabricated with two major components: cylinder and piston. Cylinder holds a volume of magneto rheological (MR) liquid. One liquid which contains of carbonyl iron elements suspended in castor oil. This liquid has shown itself to be predominantly well-suited for this application. Housing is a cylindrical pipe having one closed end with an accumulator and attachment eye connected therewith. Second or open end of the housing is closed by upper end cap. A seal is provided to prevent fluid leakage from housing. The accumulator has to account for the variation in volume existing to the liquid as additional of the piston rod come into the housing and furthermore permit for thermal expansion of the MR liquid. It also prevents cavitation effect. Piston head is spool formed having an upper and a lower outwardly extending flanges. Coil is wound upon spool-shaped piston head between upper flange and lower flange. Piston head is made of a magnetically permeable material, in this case, low carbon steel. Guide rails are attached above and below side of piston to keep the piston in centring position to housing during operation. Piston head is shaped with a smaller maximum diameter (in this case, Dpole) than the inside diameter, Di of cylinder. The outside surfaces of guides are shaped to engage the inside diameter Di of cylinder. Guides are made of non-magnetic material, in this case, bronze, and it maintains piston centred within cavity '*h*'. In this model, cavity *h* (in combination with coil) works as a valve to govern the flow of MR liquid past piston. Electrical connection is provided to coil through piston rod by two lead wires. One wire is joined to a first end of an electrically conductive rod which extends through piston rod to outside of damper. The other end of the winding of coil is attached to a "ground" connection on the outside of damper as shown in figure, the upper end of piston rod has threads to allow attachment of damper. A current in the range of 0-4 amps at a voltage of 12-24 volts is provided by connecting the leads with an external power supply. The outside surface of coil is layered with epoxy paint as a protecting measure. The damper of present experiment works as a Bingham type damper, i.e., this structure come close to an ideal damper in which the force produced is not depends on piston velocity and big forces can be produced with small or zero velocity. This independence increases controllability of the damper making the force a function of the magnetic field strength, which is a function of current flow in the circuit.

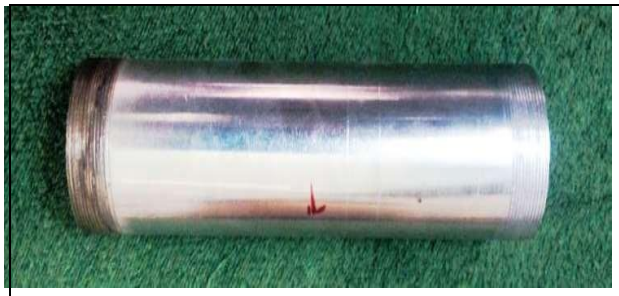

Figure5: Damper Cylinder (Housing or Shock Tube)

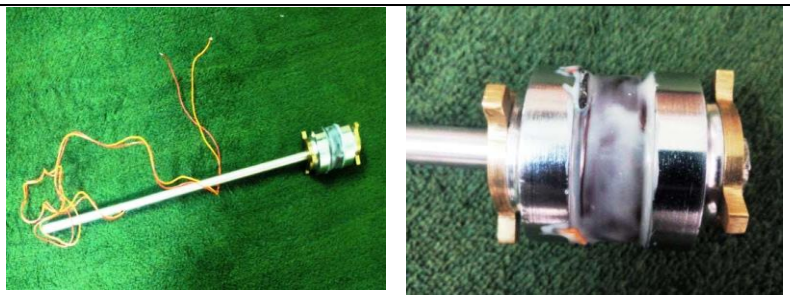

Figure 6:: Piston and Piston Rod Shown with magnetic coil and guide rail

Figure 7: Accumulator with lower end cap

Figure 8:Upper end cap with seal and filling of damper

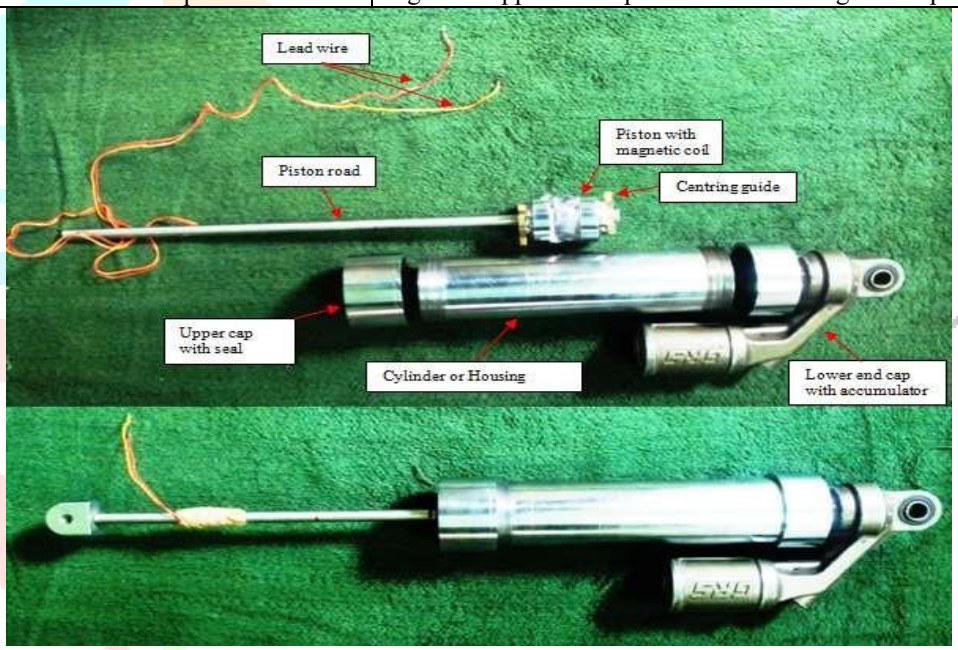

Figure 9: Assembly of Damper

IV. TESTING OF DEVLOPED MR FLUID BASE DAMPER

To investigate the fundamental behavior of the designed small-scale MR damper, a series of quasi-static experiments were conducted at the Physics Department Laboratory, Bhavnagar University. In this chapter, subsequent segments describe the experimental setup and experimental results. Results are presented for the different test carried out like variable input current tests, amplitude-dependent tests and frequency-dependent tests. The experimental results are then used to compare with theoretical results obtained using a mathematical model described in the previous chapter. The experimental results are also used to validate experiment procedure by design of experiment methodology using design expert software. Very good comparisons in force-displacement behavior are observed between theoretical and experimental results. The damper, also known as a shock absorber, is characterized by its instantaneous value of position velocity, acceleration, force, pressure, temperature, etc. and various plots among these parameters. For the measurement of listed parameters of the damper, a test rig is designed and developed. An experiment on the test rig is carried out at different speeds and loads which led to the output in terms of sinusoidal waveform on attached oscilloscope. The waveform is used to find out the characteristics at different load-speed combination. The results obtained are used to find out the behavior of damper at different speeds and loads. The principle mechanism for the basis of the experimental setup designed to measure the characteristics is single slider crank mechanism. This mechanism converts rotary motion of the circulating disc into the linear motion of the damper. At various loads and speeds combinations, the readings on the test setup is taken with the help of various sensors mounted on test rig and by using these data, characteristics of damper are evaluated. Analysis of damper could be categorized in two important headers,

(1) Rig analysis of component or complete of the damper
(2) Road analysis of the damper on the motor vehicle.

The purpose of Damper Test Rig is to construct a damper dynamometer. Damper dynamometer is an instrument to examination dampers and produce charts for the damper characteristics. These charts are made for the dampers or stored so user could develop Database of in what way every damper works under the experiment conditions. This instrument switches the trial and error methodology into a reliable and effective process to decide the damper used during an operation.

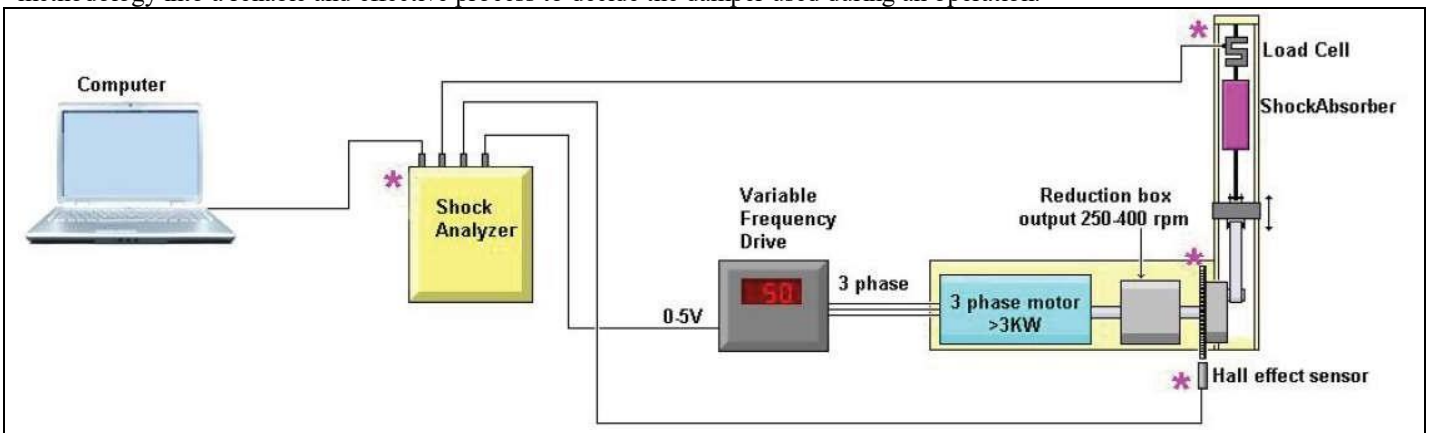

Figure 10: Experimental set up

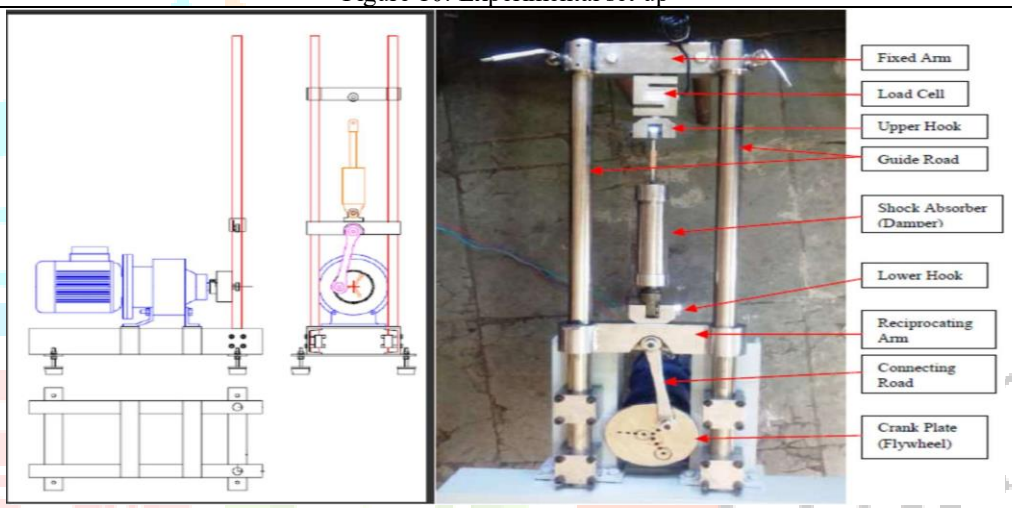

Figure 11:Test Rig for Experimentation

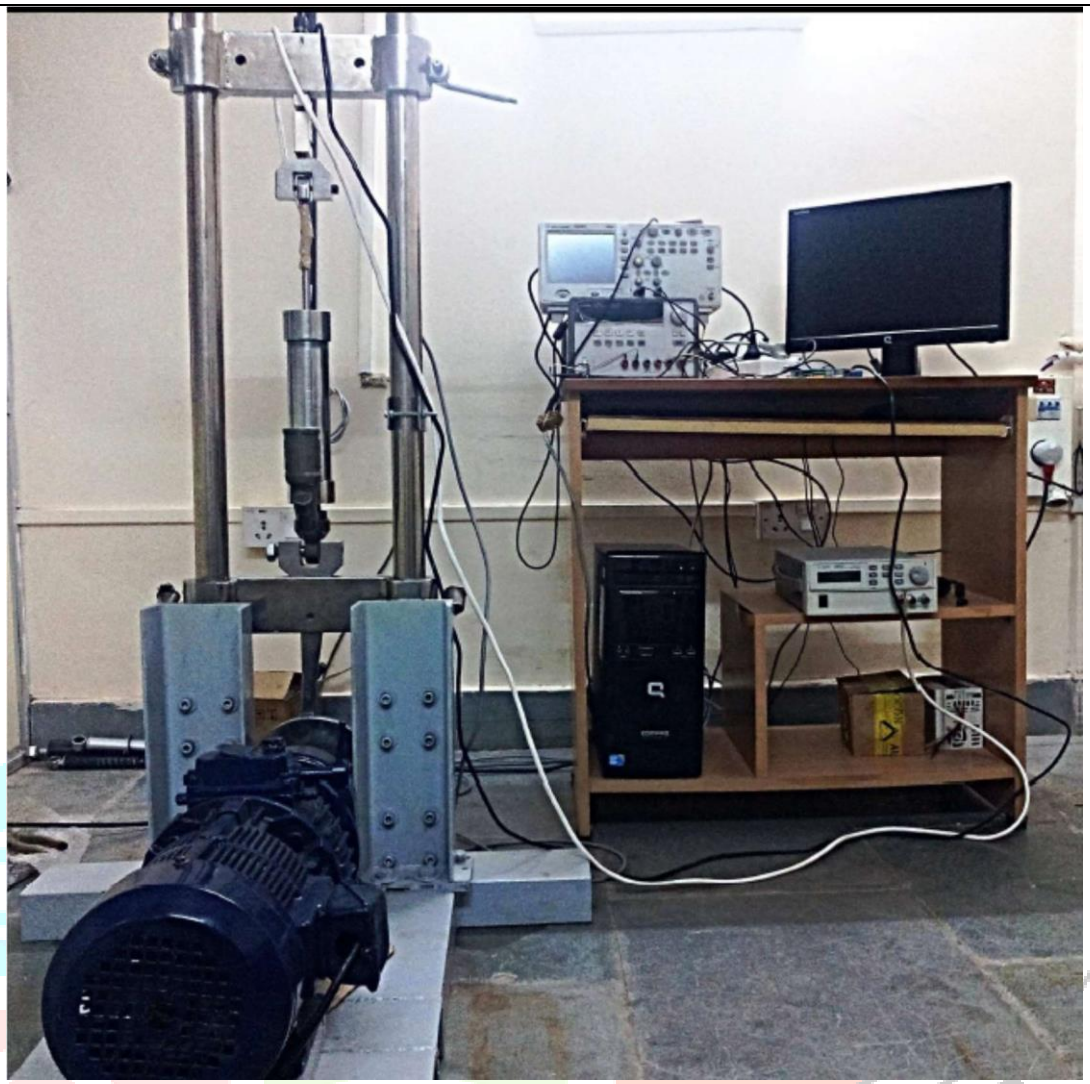

Figure 12:Fully instrumented damper test rig developed at physics department laboratory

Figure indicates fully instrumented damper test rig developed for present investigation with setup. The setup consist of piston and crank (Single Slider Crank Mechanism). This mechanism be made up of a crank, connecting rod and piston (reciprocating arm). The crank plate has holes drilled to achieve different stroke lengths. The advantage of this mechanism is its cost effectiveness because there is less high tolerance machining. The frequency is adjusted by using variable gear drive system powered by electric motor. The speed available from the motor is geared down by means of gearbox. The maximum output shaft speed is in the range of 350 to 400 RPM at full speed of motor having 1440 RPM. Variation of stroke is possible by fixing the connecting road in appropriate hole made in crank plate, as a result the stroke is fixed to provide the preferred maximum speed inside the limits of the damper and experiment apparatus. There are twelve screwed holes positioned over spiral form; connecting rod can be secure in appropriate hole to choice stroke length. The higher the stroke, the greater the power required on motor to move the damper. Dampers are fastened into the test rig on the given mounting positions. The stroke and motor speed is fixed to a selected speed choice. The computer is set to obtain the data from oscilloscope. Initial damper body temperature is taken and system is provided which keep the damper body temperature constant during experiment. The test rig is then started and the damper is operated within the selected velocity range. The data are directed to the computer via oscilloscope. The computer can then show the data in a numerical and graphical form that will permit the operator to regulate the damper accordingly.

Testing of developed MR Fluid Damper under Sinusoidal Displacement Excitations

To obtain the data used to characterize the designed MR fluid damper behavior, a series of experiments on the test rig were conducted under various sinusoidal displacement excitations while simultaneously altering the magnetic coil in a varying current range. The output of each test was the force generated by the damper. During all the experiments, the damping force response was measured together with the variation of piston displacement and supplied current for the damper. The setting parameters for experiments are listed in Table 4. Instantaneous values of time, displacement and force for complete cycle are stored in computer via oscilloscope in voltage form. Finally, the data are converted in the form of physical unit by C program developed for this special application (listed in appendix-B). Instantaneous value of velocity is calculated by differentiation of displacement with respect to time. Observations are taken according to this plane and represented in graphical form.

Table IV: Setting parameters for experiment

Amplitude	Frequency In Hz	Current Value in Amp.				
0.5 cm	0.75	0	0.25	0.5	0.75	1
	1.0	0	0.25	0.5	0.75	1
	1.5	0	0.25	0.5	0.75	1
	2.0	0	0.25	0.5	0.75	1
1.0 cm	0.75	0	0.25	0.5	0.75	1
	1.0	0	0.25	0.5	0.75	1
	1.5	0	0.25	0.5	0.75	1
	2.0	0	0.25	0.5	0.75	1
1.5 cm	0.75	0	0.25	0.5	0.75	1
	1.0	0	0.25	0.5	0.75	1
	1.5	0	0.25	0.5	0.75	1
	2.0	0	0.25	0.5	0.75	1
2.0 cm	0.75	0	0.25	0.5	0.75	1
	1.0	0	0.25	0.5	0.75	1
	1.5	0	0.25	0.5	0.75	1
	2.0	0	0.25	0.5	0.75	1

The minimum shaft rotation connected with motor via gearbox is about 40 RPM. Due to that reason, the minimum frequency value is selected as 0.75 Hz and then increased it in terms of 1.0, 1.5 and 2.0 Hz. The intermediate value is sufficient for understanding the behavior of damper with respect to frequency variation. The current value is selected from 0 Amp to 1.0 Amp. Beyond maximum limit of 1.0 Amp current value, the magnetic circuit get saturated and there will be no effect of higher current value. It is also important to study the behavior of damper at off state condition, i.e. at 0 Amp current value. Thus the range of current is selected form 0 Amp to 1.0 Amp with increment of 0.25 Amp for better understand of change in current behavior. Results of various experimental tests under sinusoidal displacement excitations are presented. These tests include: variable input current tests, frequency dependent test and amplitude-dependent tests. Force-displacement, force-velocity and force-time experiments under sinusoidal displacement excitation at different frequencies with different constant current levels of 0, 0.25, 0.5, and 1 A were conducted. At each current level, excitations with altered amplitudes and frequencies were applied to the MR damper. The tests conducted for presented damper configuration are summarized in tubular form in further part, and complete experimental results were presented in graphical form. Again, to reduce temperature effects, the tests were conducted at a temperature of 30^0C ± 3. It is also to be noted that experimental and theoretical data are presented and compared at each level. The whole experiment procedure was carried out in four steps. During each step, the value of amplitude was keep constant and for each frequency level, instantaneous values of damping force, displacement and velocity were measured for complete cycle at different values of current as shown in Table above.

Following four test were conducted for frequency ranges from 0.75 to 2 Hz

1) Test with constant amplitude value of 0.5 cm (Stroke length 1.0 cm)
2) Test with constant amplitude value of 1.0 cm (Stroke length 2.0 cm)
3) Test with constant amplitude value of 1.5 cm (Stroke length 3.0 cm)
4) Test with constant amplitude value of 2.0 cm (Stroke length 4.0 cm)

Following Table shows the experimental and analytical results variation during one complete cyclewith following parameter value.

Table V: Amplitude A= 0.5 cm. (Stroke Z = 1.0 cm.) Frequency f = 0.75 Hz. (Angular speed of crank plate = 45 RPM)

Figure 13:Force-disp. relationships under 0.5 cm amplitude for different current values at f = 0.75 Hz

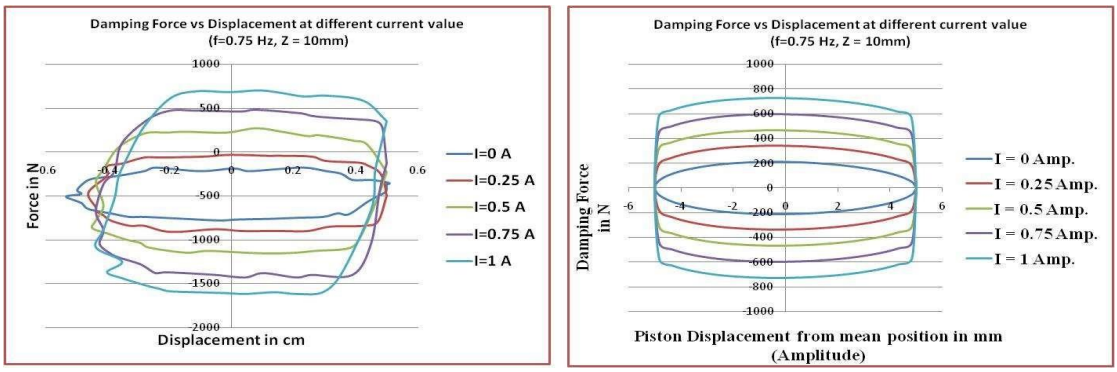

Figure 14:Force-velocity relationships under 0.5 cm amplitude for different current values at f = 0.75 Hz

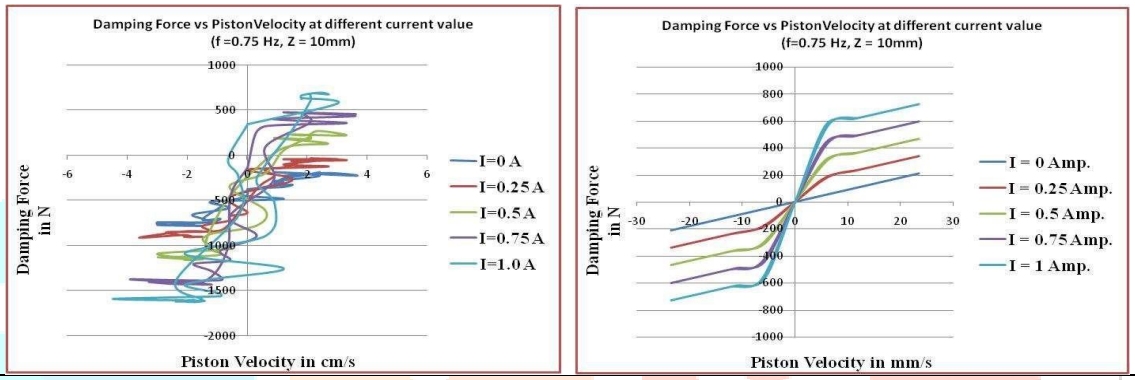

Figure 15:Force-time relationships under 0.5 cm amplitude for different current values at f = 0.75 Hz

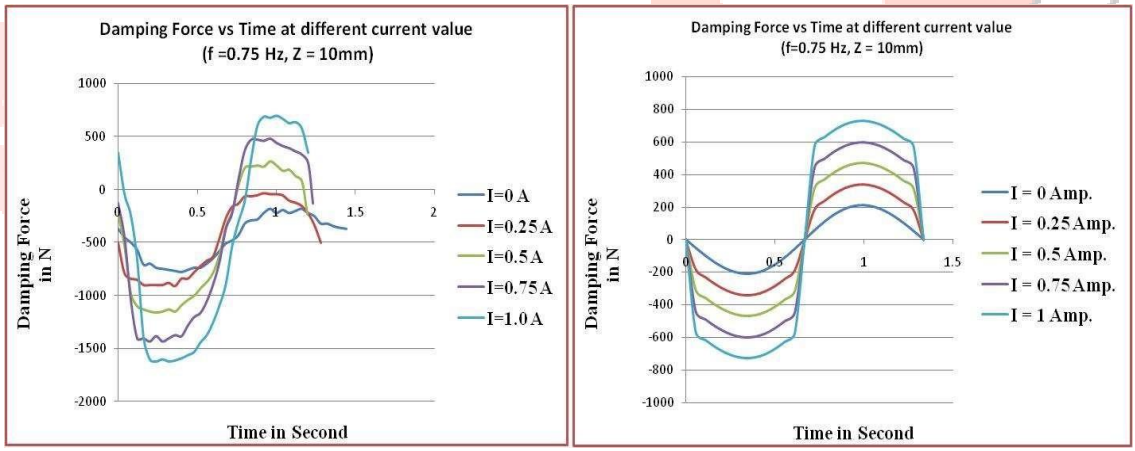

The results for varies frequencies with amplitude 0.5 cm has been tabulated below, Measured maximum force, controllable force and dynamic range and their comparison withanalytical results for the value of **Amplitude = 0.5 cm.**

			For I = 0A	For I = 0.25A	For I = 0.5A	For I = 0.75A	For I = 1A
N=45 RPM, f=0.75 Hz	Max. Force in N At 0.5 cm amp. (Span/2)	Measured	249.00	404.00	562.00	703.00	868.00
		Predicted	209.83	339.26	468.70	598.13	727.57
		Error in %	18.67	19.08	19.91	17.53	19.30
	Controllable Force in N	Measured	0.00	155.00	313.00	454.00	619.00
		Predicted	0.00	129.43	258.87	388.30	517.74
		Error in %	0.00	19.75	20.91	16.92	19.56
	Dynamic Range	Measured	0.00	0.62	1.26	1.82	2.49
		Predicted	0.00	0.62	1.23	1.85	2.47
		Error in %	0.00	0.91	1.89	1.48	0.75
			For I = 0A	For I = 0.25A	For I = 0.5A	For I = 0.75A	For I = 1A
N=60 RPM, f=1 Hz	Max. Force in N At 0.5 cm amp. (Span/2)	Measured	342.00	500.00	638.00	803.00	958.00
		Predicted	279.83	409.26	538.70	668.13	797.57
		Error in %	22.22	22.17	18.43	20.19	20.12
	Controllable Force in N	Measured	0.00	158.00	318.00	461.00	616.00
		Predicted	0.00	129.43	258.87	388.30	517.74
		Error in %	0.00	22.07	22.84	18.72	18.98
	Dynamic Range	Measured	0.00	0.46	0.99	1.35	1.80
		Predicted	0.00	0.46	0.93	1.39	1.85
		Error in %	0.00	0.12	7.42	2.86	2.65
			For I = 0A	For I = 0.25A	For I = 0.5A	For I = 0.75A	For I = 1A
N=90 RPM, f=1.5 Hz	Max. Force in N At 0.5 cm amp. (Span/2)	Measured	510.00	634.00	794.00	996.00	1151.00
		Predicted	419.65	549.09	678.52	807.96	937.39
		Error in %	21.53	15.46	17.02	23.27	22.79
	Controllable Force in N	Measured	0.00	124.00	284.00	486.00	641.00
		Predicted	0.00	129.43	258.87	388.30	517.74
		Error in %	0.00	4.20	9.71	25.16	23.81
	Dynamic Range	Measured	0.00	0.24	0.56	0.95	1.26
		Predicted	0.00	0.31	0.62	0.93	1.23
		Error in %	0.00	21.17	9.73	2.99	1.87
			For I = 0A	For I = 0.25A	For I = 0.5A	For I = 0.75A	For I = 1A
N=120 RPM, f=2 Hz	Max. Force in N At 0.5 cm amp. (Span/2)	Measured	616.00	726.00	907.00	1104.00	1263.00
		Predicted	559.57	689.00	818.44	947.87	1077.31
		Error in %	10.09	5.37	10.82	16.47	17.24
	Controllable Force in N	Measured	0.00	110.00	291.00	488.00	647.00
		Predicted	0.00	129.43	258.87	388.30	517.74
		Error in %	0.00	15.02	12.41	25.67	24.97
	Dynamic Range	Measured	0.00	0.18	0.47	0.79	1.05
		Predicted	0.00	0.23	0.46	0.69	0.93
		Error in %	0.00	22.80	2.11	14.16	13.52

Further similar process were performed for different amplitudes and varying frequencies, the summarized results has been tabulated below, Tests were conducted to investigate the effect of various parameters like amplitude, frequency and input current on MR damper performance. In these tests, various sinusoidal displacement excitations with frequencies of 0.75, 1.0, 1.5 and 2.0 Hz were selected. For each frequency, excitations with different amplitudes were applied to the MR damper at current levels of 0, 0.25, 0.5, and 1 A. The tests conducted for each amplitude value are summarized in tabular form shown

above the damper force-displacement, damper force-velocity and damper force-time relationships under different values of frequency and current. Each figure and table provides a comparison between the measured damper responses and analytical results using the axisymmetric Herschel-Bulkley model. When the displacement excitation is lesser, such as the displacement amplitude of 0.5 cm, the MR damper functions mainly in the pre-yield area. The velocity increases as the value of amplitude increases. Thus more MR fluids begin to yield, and a greater post-yield shear flow is developed. Consequently, the plastic viscous force becomes substantial, especially at large displacement amplitudes Figures show the MR damper force-displacement, force-velocity and force-time actions under a different combination values of sinusoidal displacement excitations and frequencies at various input current levels. It is concluded that resisting force increases at larger amplitudes due to higher velocity. Note that the force-displacement loops develops along a clockwise path over time, whereas the force-velocity loops develops along a counter-clockwise path over time. As shown in the figures, the force-displacement, force- velocity and force-time actions for different displacement and frequency are quite consistent. The special effects of changing input current are readily detected. At an input current of 0 A, the MR damper primarily displays the characteristics of only viscous device (i.e., the force-displacement relationship is approximately elliptical and the force-velocity relationship is approximately linear). As the input current increases, the force required to yield the MR fluid in the damper also increases and plastic-like actions are seen in the hysteresis loops. Figs. 6.6–6.21 compares the analytical values and measured values of experiments using the axisymmetric Herschel-Bulkley model. The force-displacement actions are seen to be reasonably modelled. Two extra clockwise loops are also observed at velocity extremes in the force-velocity plot. The strictions phenomenon of MR fluids (WEISS et al 1995) [52] and probably the fluid inertial force contribute to these loops as well as to force overshoots at displacement maximums. From Fig. 6.6 to 6.21 and summary Table from 6.3 to 6.6, one can also see that the maximum damping force increases when the frequency increases due to the larger plastic viscous force at higher velocity. It should also to be noted that the damper may be subjected to a small input current and a displacement excitation with a big amplitude. In these circumstances, the yield force level is low and damper functions mainly in post-yield area. Hence, as the frequency increases, the plastic viscous force starts to govern the damper reaction, especially at higher frequencies. Moreover, the effect of accumulator pressure on MR damper reaction is discussed. A pressurized accumulator is shown to be effective in decreasing the force lag due to the residual air trapped in the damper. In addition, an approach for minimizing the air in the damper during the filling method is provided.

V. RESULTS AND DISCUSSION WITH DESIGN OF EXPERIMENT

This chapter includes complete discussion on results observed during experiment. For the validation of experiment procedure, Design of Experiment (DOE) was carried out first with the help of Design Expert software using results observed during experiment. Three parameters namely amplitude, angular speed and current were selected to find out its effect on total damping force. Table 7.1 shows the parameters and their levels. Thirty two trial runs included of 23 factorial points, four centre points and five axial points were carried out in block 1. Table 7.2 shows whole design matrix with responses to total damping force. In design matrix, the coded variables are prescribed as: A: amplitude (A), B: angular speed (N) and C: current (I). F is the response representing total damping force. Experiments were conducted randomly as shown in design matrix (‘runs’ column in Table 7.2). The design matrix also show the factorial points, centre points and axial points with coded and actual values.

TABLE VI: Parameters and their levels

Factor	Unit	Low level (-1)	Centre level (0)	High level (1)
Amplitude	mm	5	10	15
Angular speed	RPM	60	90	120
Current	Amp	0	0.5	1.0

TABLE VII: Design matrix with responses (Total Damping Force)

Std	Run	Block	Type	A:A(mm)		B:N(rpm)	C:I(Amp)	A:A(mm)	B:N(rpm)	C:I(Amp)	F(N)
1	5	1	Axial	0		0	-1	10	90	0	805
2	16	1	Fact	-1		1	0	5	120	0.5	907
3	29	1	Centre	0		0	0	10	90	0.5	1080
4	14	1	Centre	0		0	0	10	90	0.5	1080
5	20	1	Fact	0		-1	1	10	60	1	1215
6	8	1	Fact	0		1	-1	10	120	0	960
7	12	1	Fact	1		-1	0	15	60	0.5	1124.5
8	13	1	Axial	-1		0	0	5	90	0.5	794
9	4	1	Fact	-1		0	-1	5	90	0	510
10	19	1	Fact	-1		-1	1	5	60	1	958
11	17	1	Axial	0		1	0	10	120	0.5	1205
12	27	1	Fact	1		1	1	15	120	1	2070
13	10	1	Fact	-1		-1	0	5	60	0.5	638
14	32	1	Centre	0		0	0	10	90	0.5	1080
15	7	1	Fact	-1		1	-1	5	120	0	616
16	30	1	Centre	0		0	0	10	90	0.5	1080
17	26	1	Fact	0		1	1	10	120	1	1492
18	18	1	Fact	1		1	0	15	120	0.5	1803
19	25	1	Fact	-1		1	1	5	120	1	1263
20	23	1	Fact	1		-1	1	10	90	1	1360
21	22	1	Fact	-1		0	1	5	90	1	1151
22	24	1	Fact	1		0	1	15	90	1	1669.5
23	11	1	Axial	0		-1	0	10	60	0.5	903
24	21	1	Fact	1		-1	1	15	60	1	1434.5
25	9	1	Fact	1		1	-1	15	120	0	1545
26	2	1	Fact	0		-1	-1	10	60	0	599
27	28	1	Fact	0		0	0	10	90	0.5	1080
28	6	1	Fact	1		0	-1	15	90	0	1155
29	1	1	Fact	-1		-1	-1	5	60	0	342
30	3	1	Fact	1		-1	-1	15	60	0	875
31	15	1	Axial	1		0	0	15	90	0.5	1397.5
32	31	1	Fact	0		0	0	10	90	0.5	1080

TABLE VIII: ANOVA (partial sum of square) for total damping force (F)

Source	Sum of squares	d.f.	Mean square	F-value	Prob>F	Remark
Model	4365178	9	485019.7354	255.865	< 0.0001	Significant
A-A-Amplitude	1930613	1	1930612.5	1018.466	< 0.0001	Significant
B-B-RPM	790443.6	1	790443.5556	416.9868	< 0.0001	Significant
C-C-Current	1505691	1	1505690.889	794.3049	< 0.0001	Significant
AB	107541.3	1	107541.3333	56.73183	< 0.0001	Significant
AC	7752.083	1	7752.083333	4.089497	0.0555	
BC	638.0208	1	638.0208333	0.336578	0.5677	
A^2	17807.78	1	17807.77502	9.394227	0.0057	
B^2	2.640405	1	2.640405294	0.001393	0.9706	
C^2	874.9481	1	874.9480976	0.461566	0.5040	
Residual	41703.38	22	1895.60825			
Lack of Fit	41703.38	17	2453.140088			
Pure Error	0	5	0			
Cor Total	4406881	31				
Std. Dev.	43.53858		R-Squared	0.990537		
Mean	1102.25		Adj R-Squared	0.986665		
C.V. %	3.949974		Pred R-Squared	0.976504		
PRESS	103545.1		Adeq Precision	67.89797		

The Model F-value of 255.862 implies that the model is significant. There is only 0.01% chance that large value of "Model F-Value" could occur due to noise. Values of "Prob > F" less than 0.05 indicate that model terms are significant. In this case A, B, C and AB are significant model terms. Values greater than 0.05 indicate that model terms are not significant. The "Pred R-Squared" of 0.976504 is in practical agreement with the "Adj R- Squared" of 0.986665. "Adeq Precision" indicates the signal to noise ratio. A ratio greater than 4 is required. The ratio of 67.89797 point out an acceptable signal. This model can be used to navigate the design space.

Results and discussion based on DOE

Table 7.2 shows all values of total damping force. The total damping force was obtained in the range of 342 N to 2070 N.

The increase in total damping force is due to:

1. Increase in applied current value increases the shear stress of MR fluid
2. Increase in angular speed increases the velocity of piston
3. Increase in amplitude. This is also due to large displacement of fluid inside the piston cylinder assembly.

Figures shows relation between total damping force (measured force in N) with applied current values, angular speed and amplitude for different combinations. The rate of increase in total damping force is higher for increasing the value of current compared to amplitude and velocity. Figure also show that the total damping force is increased linearly with respect to increase in value of applied current. This comment come to an agreement well with results described by former investigators. [13, 14, 15, 17, 20] Additionally, the results were analysed in “Design Expert V6” software. The results of the block 1 experiments in the method of analysis of variance (ANOVA) are shown. An ANOVA summary table is normally used to summarize the test of the regression model, test of the significance factors and their interaction and lack-of-fit test. If the value of ‘Prob > F’ in ANOVA table is less than 0.05 then the model, the factors, interaction of factors and curvature are said to be significant.

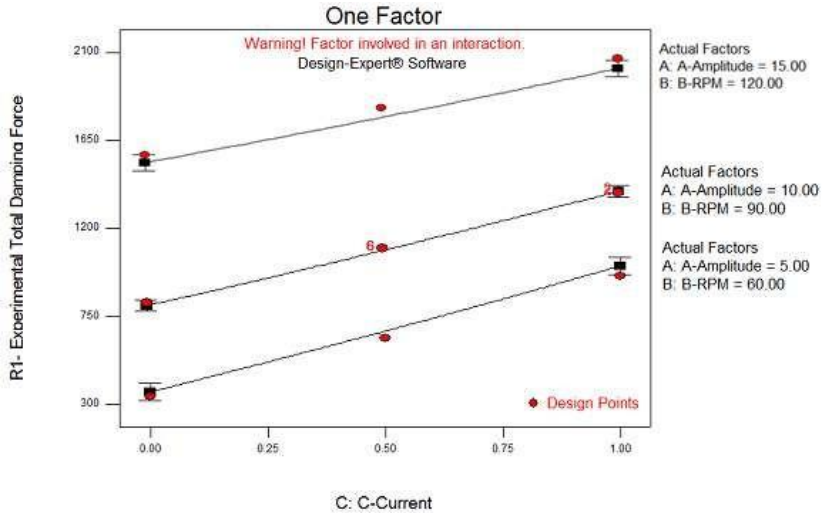

Figure 16: Total measured damping force vs. applied current at different values of amplitude and angular speed

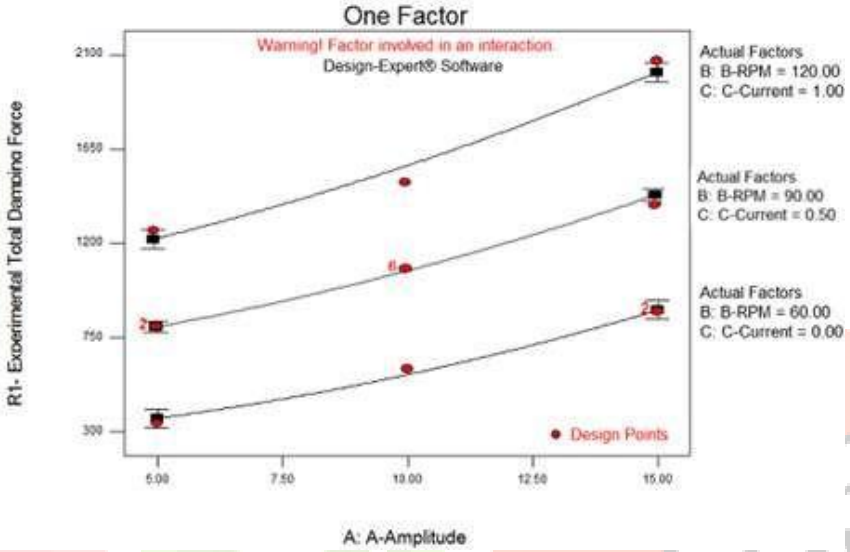

Figure 17: Total measured damping force vs. Amplitude at various angular speed and applied current.

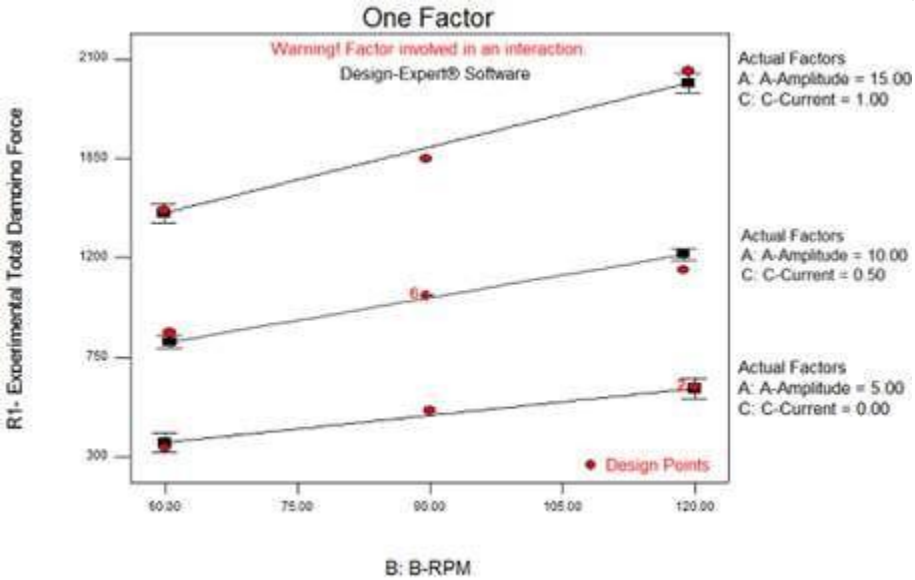

Figure 18: Total measured damping force vs. Angular velocity at various amplitude and applied current.

Table above shows that the model is significant and amplitude (A), angular speed (B), applied current (C) and (A, B) are only the important elements (terms) in the model. All remaining elements are insignificant. The influence of elements, their interaction and curvature are also presented in Table. The various R2 statistics (i.e. R2, adjusted R2 (R2 Adj) and predicted R2 (R2 Pred)) of the total damping force are shown in Table. The value of R2 = 0.990537 for total damping force indicates that 99.05% of the total variations are explained by the model. The adjusted R2 is a statistic that is adjusted for the "size" of the model; that is, the number of factors (terms). The value of the R2 Adj = 0.986665 indicates that 98.66% of the total variability is explained by the model after considering the significant factors. R2 Pred = 0.976504 is in good agreement with the R2 Adj

and shows that the model would be expected to explain 97.65% of the variability in new data (Montgomery, 2001). 'C.V.' stands for the coefficient of variation of the model and it is the error expressed as a percentage of the mean ((S.D./Mean)×100). Lower value of the coefficient of variation (C.V. = 3.9%) indicates improved precision and reliability of the conducted experiments. As nonlinearity is not existing in the model, extra tests are not necessary to be performed. This is the main benefit of sequential approach in face cantered central composite design.

The normal probability plot of the residuals (i.e. error = predicted value from model−actual value) for Total damping Force shown in Figure, reveal that the residuals lie reasonably close to a straight line, giving support that terms mentioned in the model are the only significant (Montgomery, 2001).

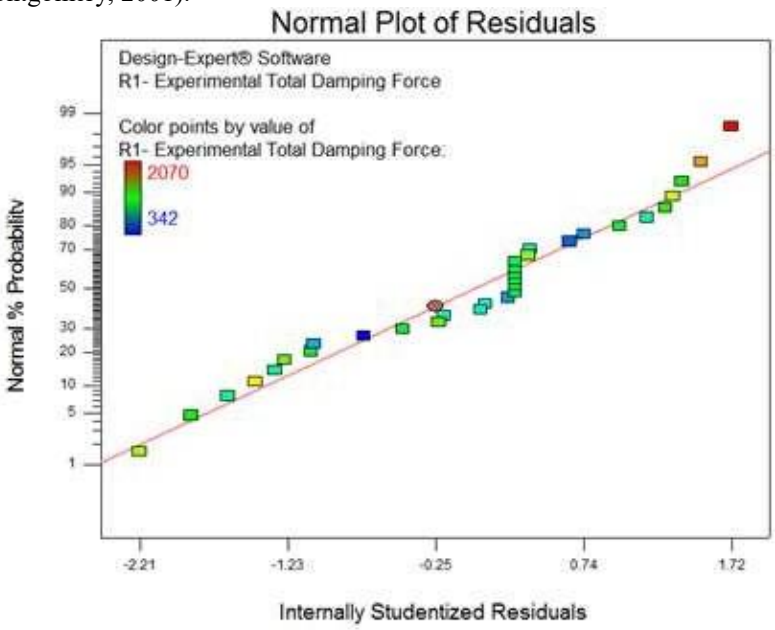

Figure 20: Normal probability plot of residuals for Total Damping Force

After eliminating the insignificant elements, the response surface equations for Total Damping Force is achieved in the real values as:

Total Measured damping Force

$$F = -26.1306 * A + 1.038635 * B + 679.6246 * C + 0.631111 * A * B - 10.1667 * A * C — 0.48611 * B * C + 1.995699 * A^2 - 0.00068 * B^2 + 44.23656 * C^2 + 195.8705$$

Where F = Total damping force in N A = Amplitude value in mm
B = Angular Speed value in RPM C = Applied Current value in Amp.

The predicted results from the model (equation value) and the real (experimental) results are presented in figure,

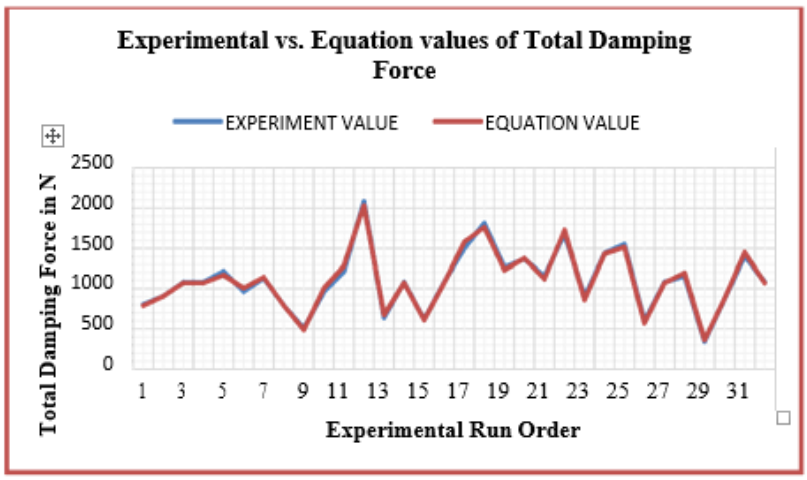

Figure 21: Actual vs. predicted values of total damping forces.

Variable damping force is required for replacing the passive vibration control system to a semi-active vibration control system. The main attention of this investigation is to find out total damping force for required damping coefficient. Therefore, the contour plots of the total damping force with relations of amplitude of vibration, angular velocity of vibrating device and applied current to MR damper are essential. The contour plot of the total damping force in angular velocity-amplitude at current value of 0.5 amp, current-amplitude at angular velocity value of 90 RPM and current-angular velocity at amplitude value of 10 mm are shown in Figs. 7.6-7.8 respectively. Figs. 7.6-7.8 clearly indication that an adequate total damping force can be attained for every level of amplitude and angular velocity when

current value is changed from low to high. In present research work, the MR fluid based semi-active damper is designed to achieve variable damping force by changing the current value.

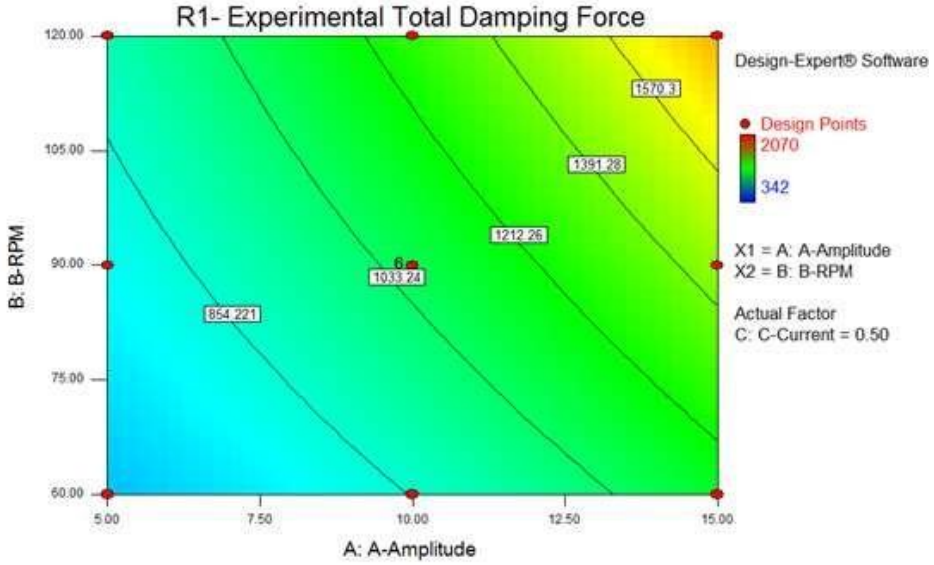

Figure 22: Measured Damping Force contour in Angular speed and Amplitude (mm) plane at current value of 0.5 Amp.

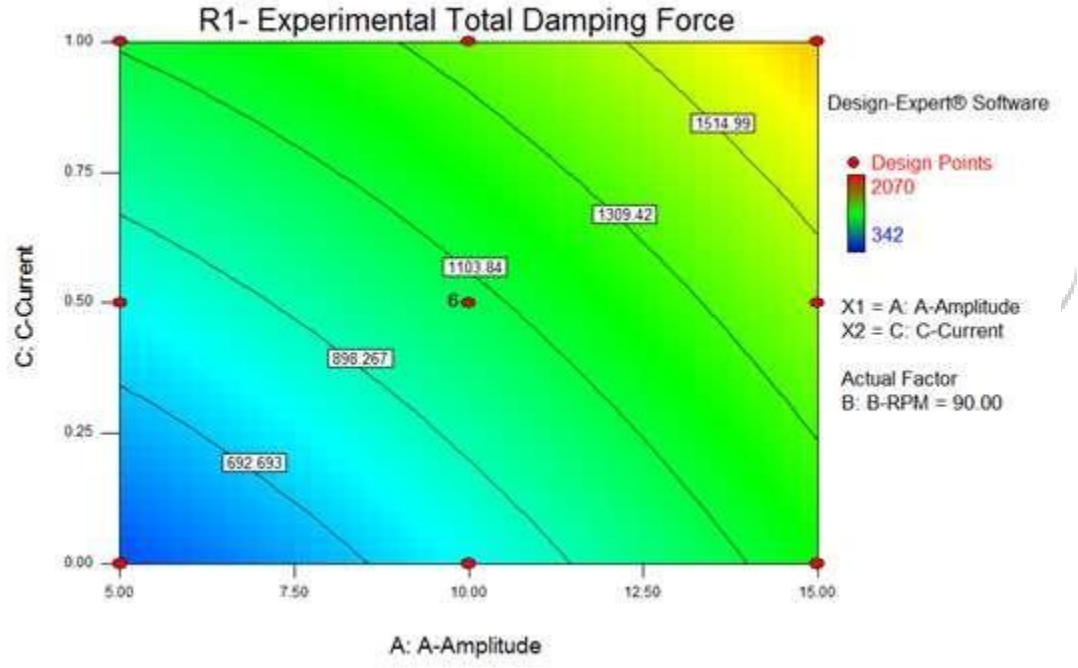

Figure 23: Measured Damping Force contour in current (Amp) and Amplitude plane at Angular speed of 90 RPM.

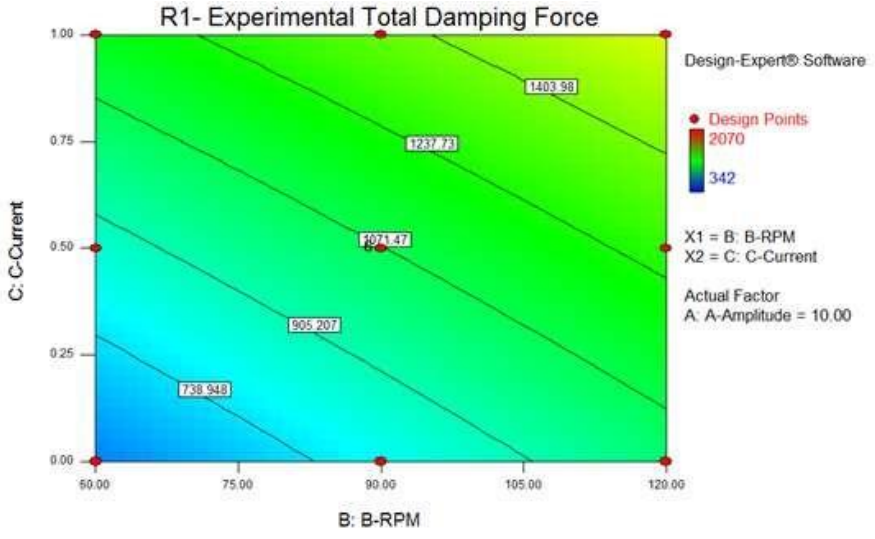

Figure 24: Measured Damping Force contour in current and Angular speed (RPM) plane at Amplitude of 10 mm.

Results and discussion based on Experimental and mathematical modelling data.

- Tests were conducted to investigate the effect of various parameters like amplitude, frequency and input current on MR damper performance. In this test, various sinusoidal displacement excitations with frequencies of 0.75, 1.0, 1.5 and 2.0 Hz were selected. For each frequency, excitations with different amplitudes were applied to the MR damper at current levels of 0, 0.25, 0.5, and 1 A. The tests conducted for each amplitude value are summarized in previous chapter by Table and Figures show the damper force-displacement, damper force-velocity and damper force-time relationships under different values of frequency and current. Each figure and table provides a comparison between the measured damper responses and analytical results using the axisymmetric Herschel-Bulkley model.
- When the displacement excitation is lesser, such as the displacement amplitude of 0.5 cm, the MR damper functions mainly in the pre-yield area. The velocity increases according to the value of amplitude increases. Thus, more MR fluid begin to yield and a greater post-yield shear flow is developed. Consequently, the plastic viscous force becomes substantial, especially at large displacement amplitudes. Figures, show the MR damper force-displacement, force-velocity and force-time actions under different combination values of sinusoidal displacement excitation and frequencies at various input current levels. It is concluded that resisting force increases at larger amplitudes due to higher velocity. Note that the force-displacement loops development takes place along with clockwise path over time, whereas the force-velocity loops development takes place along with counter-clockwise path over time. As shown in the figures, the force-displacement, force-velocity and force-time actions for different displacements and frequencies are quite consistent.
- The special effects of changing input current are readily detected. At an input current of 0 A, the MR damper primarily displays the characteristics of viscous device only. (i.e., the force-displacement relationship is approximately elliptical and the force-velocity relationship is approximately linear). As the input current increases, the force required to yield the MR fluid in the damper also increases and plastic-like actions are seen in the hysteresis loops. Figures compares the analytical values and measured values of experiment using the axisymmetric Herschel-Bulkley model. The force-displacement actions are reasonably observed for the purpose of modelling. Two extra clockwise loops are also observed at velocity extremes in the force-velocity plot. The strictions phenomenon of MR fluid (Weiss et al 1995) [52] and probably the fluid inertial force contribute to these loops as well as to force overshoots at displacement maximums.
- From Figures and summary Table one can also see that the maximum damping force increases when the frequency increases due to the larger plastic viscous force at higher velocity. It should also to be noted that the damper may be subjected to a small input current and a displacement excitation with big amplitude. In this circumstances, the yield force level is low and damper functions mainly in post-yield area. Hence, as the frequency increases, the plastic viscous force starts to govern the damper reaction especially at higher frequencies. Moreover, the effect of accumulator pressure on MR damper reaction is discussed. A pressurized accumulator is seen effective to decreasing the force lag due to the residual air trapped in the damper. In addition, an approach for minimizing the air in the damper during the filling method is provided. As can be seen, the MR damper resisting force increases as the applied current increases. Moreover, the area enclosed by the force-displacement loop also enlarges and more energy is dissipated. Figures provide the measured MR damper force-velocity behaviours and comparisons with theoretical results. Due to the plastic viscous force, a larger damping force is seen at high velocity. Figures provide the measured MR damper force-time behaviours and comparisons with theoretical results. Tables provides the measured maximum damping force, controllable force and dynamic range with their comparison to analytical results. Again, close agreement is observed with maximum errors of about 10%.

MR fluid damper characteristic analysis

To design appropriate MR fluid damper model, examination of elements which affect the dynamic responses of the damping system has been done. The first affecting element is the applied displacement/velocity on the piston rod of the damper. Figure shows a comparison amongst damping results under various sine excitations with 0.5, 1.0, 1.5 and 2.0 cm amplitude and frequency 0f 0.75, 1.0, 1.5 and 2.0 Hz under the provided current level in range commencing 0 to 1A. Outcomes display that at fixed current level applied to the damper, the damping force fluctuates because of the change in piston rod velocity affected by the simultaneous variation of frequency and/or amplitude of the applied excitation. The second element affecting the damper behaviour is the change in current applied to the damper coil.

It is readily apparent that:

1) The force produced by the damper is not centred at zero. This effect is due to the effect of an accumulator containing high pressure nitrogen gas in the damper. The accumulator helps to prevent cavitation in the fluid during normal operation and accounts for the volume of fluid displaced by the piston rod as well as thermal expansion of the fluid.
2) Greater the current level, greater is the damping force. Increasing the current in the device's coil enlarges the magnetic field flux and thus, increases the yield stress denoted as r0(B) as shown in Figure, increases the controllable force and the dynamic range.
3) The alteration amount of force is more rapidly at lesser current levels due to the effect of magnetic field saturation. With respect to the above examines, it is clear that the damping force of the MR fluid damper be influenced by the displacement/velocity of the damper piston and the current supplied for the coil inside the damper.

4) Referring to Table, MR damper with low frequency and high current value have higher dynamic ranges. Dynamic range is increased by increasing current value which increased controlled force up to saturation state. By increasing value of frequency, instantaneous value of velocity is increased which increased viscous force or uncontrolled force and reduction in dynamic range.
5) As shown in Figure, the magnetic field is almost saturated at the input current level of 1 A for MR fluid used for this investigation of MR damper; only very small increase in yield stress is observed when the input current increases from 0.9A to 1A. However, the yield stress increase is more noticeable in the current range of 0.2A to 0.8A, which is also effect of the material of cylinder housing; in this case it is low carbon steel.
6) With the help of mathematical model, if gap size for damper is increased, large gap size reduces the magnetic field due to its larger magnetic resistance. Consequently, it reduces the yield stress of the MR fluid; it assumes that the materials used in the magnetic loop are the same. This also implies that the use of proper material. In this investigation, it is low carbon steel having high conductive permeability increases the magnetic field in the gap at a high current level. This results in an increased yield stress. Moreover, these configurations also exhibit reduced damping forces due to their geometry.
7) From Figure (measured), force overshoots are clearly seen at the displacement extremes, where the velocity changes its direction. These overshoots appear to be primarily due to the stiction phenomenon found in MR fluids. Because large acceleration occurs at these points due to the velocity discontinuity of the sinusoidal displacement excitation, other effects such as fluid inertial force may also be contributed to these overshoot.
8) The predicted and measured values of damping forces controllable force and dynamic range are differing about ±10%. This is due to the assumed simplifications of the phenomena connected with the operation of the device, revealed a major influence on the computational inaccuracies. This effect may also be related to the simplifications in calculation of the pressure drop.
9) Precise computations of the magnetic induction are complicated, while the accurate experimental research is time and effort consuming. The r0(B) function provided by the manufacturer of the MR fluid is usually approximate and imprecise which negatively influence the accuracy of the computations. It is experimentally concluded that the maximum damping force varies linearly as the value of the yield stress varies. Difficulties in determining the magnetic induction value explain the high variation of the error. The most accurate calculations can be obtained for the smallest gap height due to the possibilities of the precise determination of the magnetic field and the small error of the simplified model of the flow between parallel plates.
10) All factors related to objectives of present research project are defined earlier in this paper and are achieved positively. MR fluid is prepared and tested with rheometer available in the laboratory of physics department, M. K. Bhavnagar University and the output is shown in Figure All the parameters are studied carefully related with MR damper design and finally a prototype of MR damper is designed and fabricated. Investigation is carried out by mathematical modelling and experiments on proto type MR damper test rig which has been designed and developed at this laboratory. Design of Experiment also carried out for validation of experiment procedure and the results of DOE is quite satisfactory.

VI. CONCLUSIONS AND FUTURE SCOPE

Conclusions:

In present research work, physical occurrences of a MR fluid base damper has been carefully examined through both experimental data and modelling methodologies. The test rig with the MR fluid damper has been fabricated appropriate to design the model in addition to assess the projected damper. The assumed simplifications of the phenomena connected with the operation of the device, revealed a major influence on the computational inaccuracies. It can be concluded that the most accurate calculations can be obtained for the smallest gap height, due to the possibility of the precise determination of the magnetic field and the small error of the simplified model of the flow between parallel plates. The analysis suggests the need to develop more precise tools supporting the design process of the devices with MR fluids. It seems reasonable to create a reverse algorithm that will allow estimation of the geometry of the device based on the desired value of the dissipated energy. In addition it is necessary to determine more accurately the value of the magnetic induction in the flow gap of the MR device. It would be also interesting to define the influence of the temperature on the viscosity and the yield stress, as well as to take this influence into account for the theoretical calculations. Various tests have been carried out using a test rig to verify the damping characteristics of developed MRF dampers. The following test results are obtained:

1) The damper functioned by using a unit of the electromagnet under an appropriate electrical current control
2) The magnitude of the damping force depends on the input magnetic field but it has an upper limit
3) In the absence of an applied magnetic field, an MRF damper exhibits viscous like behaviour, while it shows friction-like behaviour in a magnetic field.

Through a series of experiments, it is confirmed that the behaviour of the MRF damper is fairly predicted by the velocity-displacement and velocity-force relationship over a wide range of applied current, amplitude and frequency. It is clarified that the MRF dampers provide a technology that enables effective semi-active control in real development of various structures.

Future Scope

During the course of present study, a number of additional considerations and concepts be present. These possibly will be established into opportunities for forthcoming study, are point out as:

1) The present investigation was directed assuming steady-state situations. In exercise, on the other hand, fluid flow inside a specific passage is rarely steady- state. Quite the reverse, the flow is mostly transient by means of a lot of variations in flow direction and flow velocity. For example, the study of current helps to recognize behaviour under adverse steady-state circumstances. An addition would be toward consist of adverse, non-steady circumstances.
2) The MR fluid utilized for present investigation was developed in house at Physics Department, Shri M K Bhavnagar University, and Bhavnagar. This specific fluid consumed an iron particles of 40% by volume in castor oil. Forthcoming studies might reflect the influence of iron content on the behaviour of the fluid when it operates with damper.
3) Forthcoming effort may also consist of to recognize the dependency of normalized yield stress on magnetic field strength. It comprise several supplementary tests done at different magnetic field strengths. With adequate records to characterize the magnetic field dependency, it may be probable to redevelop the suggested model designed for the normalized yield stress such that this one be able to express clearly as a function of dwell time and magnetic field strength.
4) Recognize a model for the response time of MR fluid as a function of magnetic field strength.
5) Examine the dependency of particle dimensions and form on behaviour of MR fluid.
6) Examine the influence of the off-state behaviour with respect to on-state behaviour..
7) Examine the temperature effect on overall performance of MR fluid base damper.

References

[1]. "Solutions in Energy absorption and vibration isolation", Enidine Incorporated, NY-14127, USA.

[2]. Jie Gao and Ke Chen (2011), "Frequency-Domain Simulation and Analysis of Vehicle Ride Comfort based on Virtual Proving Ground", International Journal of Intelligent Engineering and Systems, Vol.4, No.3, 2011.

[3]. John C. Dixon (2007), The Shock Absorber Handbook, John Wiley & Sons Ltd. [4]. J. David Carlson, "Magnetorheological fluids – ready for real-time motion control", Lord Corporation, Materials Division, Cary, North Carolina, USA

[5]. M. R. Jolly, J. W. Bender and J. D. Carlson (1999), "Properties and Applications of Commercial Magnetorheological Fluids", Journal of Intelligent Material Systems and Structures, Vol. 10, No. 1, 1999, 5-13.

[6]. Inman D J (2006), Vibration with control, Wiley, Chichester.

[7]. De Silva CW (2006), Vibration: fundamentals and practice, 2nd edition. CRC Press, Boca Raton.

[8]. Katu U.S., Desavale R.G. and Kanai R.A., "Effect Of Vehicle Vibration on Human Body – RIT Experience", Department of Mechanical Eng., Rajarambapu Institute of Technology, Sakharale-415414.

[9]. Hiromichi Nozaki (2004), "Technology for Measuring the Damping Force of Shock Absorbers and the Constant of Coil Springs Mounted on a Motorcycle by the Un-sprung Mass Vibration Method", SAE Automotive Dynamics, Stability & Controls Conference and Exhibition, May 4-6, 2004.

[10]. Dr. Faramarz Gordaninejad (2011), "A novel magnetorheological shock absorber for vibration control", Department of the army, Army research office, February 2001.

[11]. E. Switonski, A. Mezyk, S. Duda, S. Kciuk (2007), "Prototype magnetorheological fluid damper for active vibration control system", Journal of Achievements in Materials and Manufacturing Engineering, Volume 21, Issue 1, March 2007.

[12]. Tjahjo Pranoto, Kosuke Nagaya and Atsushi Hosoda (2004), "Vibration suppression of plate using linear MR fluid passive damper", Journal of Sound and Vibration 276 (2004) 919–932.

[13]. M. R. Jolly, J. D. Carlson and B. C. Munoz (1996), "A Model of the Behaviour of Magnetorheological Materials", Smart Materials and Structures, Vol. 5, 1996, 607-614.

[14]. Miao Yu, X.M.Dong, S.B.Choi and C.R.Liao (2009), "Human simulated intelligent control of vehicle suspension system with MR dampers", Journal of Sound and Vibration 319 (2009) 753–767

[15]. R V Upadhyay, Zarana Laherisheth and Kruti Shah (2004), "Rheological properties of soft magnetic flake shaped iron particle based magnetorheological fluid in dynamic mode", Smart Mater. Struct. 23 (2014) 015002 (8pp)

[16]. J. D. Carlson and M. R. Jolly (2000), "MR Fluid, Foam and Elastomer Devices", Mechatronics, Vol. 10, Nos. 4-5, 2000, 555-569.

[17]. J Wang and G Meng (2001), "Magnetorheological fuid devices: principles, characteristics and applications in mechanical engineering", Proc Instn Mech Engrs Volume 215 Part L.

[18]. Juan de Vicente (2013): Magnetorheology: a review, Vicente, e-rheo-iba, 1 (2013) 1-18

[19]. "MRF-132DG Magneto-Rheological Fluid", Lord technical data, Lord Corporation, 2011, www.lord.com.

[20]. M. A. Golden, J. C. Ulicny, K. S. Snavely and A. L. Smith (2005), "Magnetorheological, Fluids", US Patent 6932917.

[21]. Priyank Prakash and Ashok Kumar Pandey (2015), "Performance of MR damper based on experimental and analytical modelling", The 22nd International Congress of Sound and Vibration, ICSV22, Florence, Italy, 12-16 July 2015.

[22]. J. A. Starkovich and E. M. Shtarkman (2003), "High Yield Stress Magnetorheological Material for Spacecraft Applications", US Patent 6610404.

[23]. J. Claracq, J. Sarrazin and J. Monfort (2004), "Viscoelastic properties of magnetorheological fluids", Rheol Acta 43: 38–49.

[24]. H. J. Choi, I. B. Jang, J. Y. Lee, A. Pich, S. Bhattacharya, and H.-J. Adler (2005), "Magnetorheology of Synthesized Core–Shell Structured Nanoparticle", IEEE Transactions on magnetics, Vol. 41, NO. 10, OCTOBER 2005.

[25]. N. M. Wereley, A. Chaudhuri, S. Jhon, S. Kotha, A. Suggs, R. Radhakrishnn, B.
J. Love and T. S. Sudarshan (2006), "Bidisperse Magnetorheological Fluids using Fe Particles at Nanometer and Micron Scale", Journal of Intelligent Material and Structures, Vol. 17, 2006, 393-401.

[26]. T. Shiraishi, S. Morishita and H. P. Gavin (2004), "Estimation of Equivalent Permeability in Magnetorheological Fluid Considering Cluster Formation of Particles", Journal of Applied Mechanics, Transactions of the ASME, Vol. 71, No. 2, 2004, 201-207.

[27]. Seung-Bok Choi and Young-Min Han (2013), Magnetorheological Fluid Technology, CRC Press.

[28]. E. Lemaire, Y. Grasselli and G. Bossis (1992), "Field Induced Structure in Magneto and Electro-Rheological Fluids", Journal De Physique II, Vol. 2, 1992, 359-369.

[29]. Weijia Wen, Xianxiang Huang and Ping Sheng (2008), "Electrorheological fluids: structures and mechanisms", Soft matter, 2008, 4, 200–210/201.

[30]. B. C. Munoz, G. W. Adams, V. T. Ngo and J. R. Kitchin (2001), "Stable Magnetorheological Fluids", US Patent 6203717.

[31]. C. Fang, B. Y. Zhao, L. S. Chen, Q. Wu, N. Liu and K. A. Hu (2005), "The Effect of the Green Additive Guar Gum on the Properties of Magnetorheological Fluid", Smart Materials and Structures, Vol. 14, No. 1, 2005, N1-N5.-not matched
[32]. S. Elizabeth Premalatha, R. Chokkalingam and M. Mahendran (2012), "Magneto Mechanical Properties of Iron Based MR Fluids", American Journal of Polymer Science 2012, 2(4): 50-55
[33]. J. Rabinow (1951), "Magnetic Fluid Torque and Force Transmitting Device", US Patent 2575360.
[34]. W. A. Gross (1961), "Valve for Magnetic Fluids", US Patent 3010471. [35]. J. Rabinow (1954), "Magnetic Fluid Shock Absorber", US Patent 2667237. [36]. E. Germer (1954), "Magnetic Valve", US Patent 2670749.
[37]. Seval Genc¸ and Pradeep P Phule, Rheological properties of magnetorheological fluids, Smart Mater. Struct. 11 (2002)140–146.
[38]. J. D. Carlson (2002), "What Makes a Good MR Fluid?", Journal of Intelligent Material Systems and Structures, Vol. 13, Nos. 7-8, 2002, 431-435.
[39]. P. P. Phule (1999), "Magnetorheological Fluid", US Patent 5985168, Nov-1999. [40]. J.D.Carlson, D.M.Catanzarite and K.A.St. Clair (1995), "Commercial magnetorheological fluid devices", 5th Int. Conf. on Electro-Rheological, Magneto-Rheological Suspensions and Associated Technology Sheffield, 10-14 July 1995
[41]. D. Srikala, V. N. Singh, A. Banerjee and B. R. Mehta, "Effect of induced shape anisotropy on magnetic properties of ferromagnetic cobalt nanocubes", School of Physical Sciences, Jawaharlal Nehru University, New Delhi 110067, India
[42]. C.C. Ekwebelam and H.See (2008), "Determining the flow curves for an Inverse Ferrofluid", Korea-Australia rheological journal, Vol. 20, no.1, March 2008, pp. 209-224.
[43]. Egon Krause (2005), Fluid Mechanics with Problems and Solutions, ISBN 3- 540-22981-7 Springer Berlin Heidelberg New York.
[44]. S. J. Dyke, B. F. Spencer Jr., M. K. Sain and J. D. Carlson (1996), "Modelling and Control of Magnetorheological Dampers for Seismic Response Reduction", August 1, 1996.
[45]. P Sunthar, "Polymer Rheology", Department of Chemical Engineering, Indian Institute of Technology (IIT) Bombay, Mumbai 400076 India.
[46]. AP Poloski, JJ Toth and JM Tingey (2009), "Deposition Velocities of Non- Newtonian Slurries in Pipelines: Complex Simulant Testing", U.S. Department of energy, PNNL-18316, WTP-RPT-189 Rev. 0, 2009.
[47]. K. Toda and H. Furuse (2006), "Extension of Einstein's Viscosity Equation to That for Concentrated Dispersions of Solutes and Particles", Journal of Bioscience and Bioengineering, Vol. 102, No. 6, 2006, 524-528.
[48]. Xiaocong Zhu, Xingjian Jing and Li Cheng (2012), "Magnetorheological fluid dampers: A review on structure design and analysis", Journal of Intelligent Material Systems and Structures, 0(0) 1-35.
[49]. C. Wu, Y. C. Lin and D. S. Hsu (2008), "Performance test and mathematical model simulation of MR damper", The 14th World Conference on Earthquake Engineering October 12-17, 2008, Beijing, China.
[50]. T. Butz and O. von Stryk (2002), "Modelling and Simulation of Electro- and Magnetorheological Fluid Dampers", Zeitschrift Fur Angewandte Mathematik Und Mechanik, Vol. 82, 2002, 3-20.
[51]. Bong Jun Park, Fei Fei Fang and Hyoung Jin Chi (2010), "Magnetorheology: Materials and application", Soft Matter, 2010, 6, 5246–5253, The Royal Society of Chemistry.
[52]. J. D. Carlson and K. D. Weiss (1995), "Magnetorheological Materials Based on Alloy Particles", US Patent 5382373.
[53]. R. T. Foister (1997), "Magnetorheological Fluids", US Patent 5667715.
[54]. G. Bossis, O. Volkova, S. Lacis and A. Meunier (2002), "Magnetorheology: Fluids, Structures and Rheology", Stefan Odenbach (Ed.): LNP 594, pp. 202– 230.
[55]. T. M. Simon, F. Reitich, M. R. Jolly, K. Ito and H. T. Banks (2001), "The Effective Magnetic Properties of Magnetorheological Fluids", Mathematical and Computer Modelling, Vol. 33, Nos. 1-3, 2001, 273-284.
[56]. R. H. Davis, Y. Zhao, K. P. Galvin and H. J. Wilson (2003), "Solid-Solid Contacts Due to Surface Roughness and Their Effects on Suspension Behaviour", Philosophical Transactions. Series A, Mathematical, Physical, and Engineering Sciences, Vol. 361, No. 1806, 2003, 871-894.
[57]. N. P. Sherje and Dr. S. V. Deshmukh (2016), "Preparation and Characterization of Magnetorheological Fluid for Damper in Automobile Suspension", International Journal of Mechanical Engineering and Technology, 7(4), 2016, pp. 75–84.
[58]. B. F. Spencer Jr., S. J. Dyke, M. K. Sain and J. D. Carlson (1997)," Phenomenological Model of a Magnetorheological Damper", Journal of Engineering Mechanics, ASCE, 123:230–238.
[59]. Phillips, R.W. (1969), Engineering applications of fluids with a variable yield stress, Ph.D. thesis, University of California, Berkeley, California.
[60]. "Designing with MR Fluids", ENGINEERING NOTE, Lord Corporation,
December-1999
[61]. M. Raju, N. Seetharamaiah, A.M.K. Prasad and M.A. Rahman (2016), "Experimental Analysis of Magneto-Rheological Fluid (MRF) Dampers under Triangular Excitation", International Journal of Mechanical Engineering and Technology, 7(6), 2016, pp. 284–295.
[62]. Honghui Zhang, Changrong Liao, Weimin Chen and Shanglian Huang, "A Magnetic Design method of MR fluid dampers and FEM analysis on magnetic saturation", http://www.paper.edu.cn
[63]. Guangqiang Yang, B.S., "Large-scale Magnetorheological Fluid Damper for Vibration Mitigation: Modeling, testing and Control", Ph.D. thesis, University of Notre Dame, Notre Dame, Indiana, December-2001.
[64]. Jacek Mateusz Bajkowski (2012), "Design, analysis and performance evaluation of the linear magnetorheological damper", acta mechanica et automatica, vol.6 no.1.
[65]. "Carbonyl Iron Powder", BASF-The chemical company.
[66]. Jason P. Rich, Patrick S. Doyle and Gareth H. McKinley, "Magnetorheology in an aging, yield stress matrix fluid", Massachusetts Institute of Technology, Department of Chemical Engineering, Cambridge, MA USA.
[67]. Weiss et al. (1999), "Method and Magnetorheological Fluid formulation for increasing the output of a Magnetorheological Fluid device", US Patent 5900184.
[68]. Daniel E. Barber and J. David Carlson, "Performance Characteristics of MR Fluid Engine Mounts", LORD Corporation, Cary, NC USA.
[69]. F D Goncalves and J D Carlson (2009), "An alternate operation mode for MR fluids—Magnetic Gradient Pinch", Journal of Physics: Conference Series 149 (2009) 012050.
[70]. Saiful Amri Bin Mazlan (2008), The behaviour of Magnetorheological Fluid in squeeze mode, Ph.D. thesis, Dublin City University, August-2008.
[71]. Changsheng Zhu, David A. Robb and David J. Ewins, "A Magneto-rheological Fluid Squeeze Film Damper for Rotor Vibration Control", Department of Mechanical Engineering, Imperial College, London, SW7 2BX, UK.
[72]. Carlson (1996), "Multi-degree of freedom Magnetorheological device and system for using same", US Patent 5492312.
[73]. More Thomas AVRAAM (2009), MR-fluid brake design and its application to a portable muscular rehabilitation device, Ph.D. thesis, Active Structures Laboratory Department of Mechanical Engineering and Robotics, November- 2009.
[74]. Biedermann (2002), "Leg prosthesis with an artificial knee joint provided with an adjustment device", US Patent 6423098, July-2002.
[75]. Biedermann et al. (2004), "Leg prosthesis with an artificial knee joint and method for controlling a leg prosthesis", US Patent 6755870, Jun-2004.
[76]. Webb (1998), "Exercise apparatus and associated method including rheological fluid brake", US Patent 5810696, Sep-1998.
[77]. RHEO KNEE-3, Technical Manual, OSSUR life without limitation, www.ossur.com, 2015.
[78]. Deffenbaugh et al. (2001), "Electronically prosthetic control", US Patent US 2001/0029400 A1, Oct-2001.
[79]. Junji Furusho, Takehito Kikuchi and Miwa Tokuda (2007), "Development of Shear Type Compact MR Brake for the Intelligent Ankle-Foot Orthosis and Its Control", 10th international conference on rehabilitation robotics, Noordvijk, Netherlands.

[80]. Yuhei Yamaguchi, Junji Furusho, Kenichi Koyanagi and Shinya Kimura (2003), "Development of 2-D Force Display System Using MR Actuators", ICAT, Tokyo, Japan.
[81]. D. I. Lalwani, N. K. Mehta and P. K. Jain (2008), "Experimental investigations on cutting parameters influence on cutting forces and surface roughness in finish hard turning of MDN250 steel", Journal of materials processing technology, 206 (2008), I67-I79.
[82]. Septimiu George Luca, Florentina Chira and Victor Octavian Rosca (2005), "Passive, active and semi active control systems in civil engineering", Bul. Inst. Polit. Iasi.
[83]. A. G. Olabi and A. Grunwald, "Design and Application of Magneto-Rheological Fluid – MRF", Dublin City University, School of Mechanical and Manufacturing Engineering, Glasnevin, Dublin 9, Ireland.
[84]. H. F. Lam, C. Y. Lai, and W. H. Liao, "Automobile suspension systems with MR fluid dampers", smart materials and structures laboratory, Department of mechanical and automobile engineering, The Chinese University of Hong Kong.
[85]. Bhau K. Kumbhar and Satyajit R. Patil (2014), "A Study on Properties and Selection Criteria for MagnetoRheological (MR) Fluid Components", International Journal of ChemTech Research, Vol.6, No.6, pp3303-3306, Aug- Sep 2014.
[86]. Terje O. Espelid (2003), "Doubly Adaptive Quadrature Routines based on Newton-Cotes rules", BIT Numerical Mathematics, 43:319-337, 2003.